# Mild therapeutic hypothermic protection activates the PI3K/AKT signaling pathway to inhibit TRPM7 and suppress ferroptosis induced by myocardial ischemia-reperfusion injury

YAQI LI[1,2*], YIXUAN CHEN[3*], PENG YU[4], DEJU ZHANG[5], XIAOYI TANG[3], ZICHENG ZHU[3], FAN XIAO[3], WEI DENG[3], YANG LIU[3], ZHAOYING TAN[3], JING ZHANG[3] and SHUCHUN YU[3]

[1]Jiangxi Medical College, Nanchang University, Nanchang, Jiangxi 330006, P.R. China; [2]Department of Anesthesiology, Jiangxi Provincial People's Hospital, The First Affiliated Hospital of Nanchang Medical College, Nanchang, Jiangxi 330006, P.R. China; [3]Department of Anesthesiology, The Second Affiliated Hospital of Nanchang University, Nanchang, Jiangxi 330006, P.R. China; [4]Department of Metabolism and Endocrinology, The Second Affiliated Hospital of Nanchang University, Jiangxi, Nanchang 330006, P.R. China; [5]Food and Nutritional Sciences, School of Biological Sciences, The University of Hong Kong, Hong Kong, SAR, P.R. China

Received April 3, 2024; Accepted September 4, 2024

DOI: 10.3892/mmr.2024.13345

**Abstract.** The present study aimed to investigate the role of PI3K-mediated ferroptosis signaling induced by mild therapeutic hypothermia (MTH), which was defined as a temperature of 34˚C, in protecting against myocardial ischemia-reperfusion (I/R) injury (MIRI). To meet this aim, H9C2 cells underwent hypoxia-reperfusion (H/R) and/or MTH. The MTT assay was used to assess cell viability, cytotoxicity was measured using a lactate dehydrogenase cytotoxicity assay, and Annexin V-FITC/PI flow cytometric analysis was used to analyze early and late cell apoptosis. In addition, 84 healthy adult male Sprague-Dawley rats were randomly divided into seven groups (n=12), and underwent I/R and various treatments. Hemodynamics were monitored, and the levels of myocardial injury marker enzymes and oxidative stress markers in myocardial tissue were measured using ELISA. The expression levels of PI3K, AKT, transient receptor potential cation channel subfamily M member 7 (TRPM7), glutathione peroxidase 4 (GPX4) and acyl-CoA synthetase long chain family member 4 (ACSL4) in animals and cells were measured using western blot analysis. These experiments revealed that MTH could effectively reduce myocardial infarct size, improve hemodynamic performance following MIRI and suppress myocardial apoptosis, thereby contributing to the recovery from H/R injury. Mechanistically, MTH was revealed to be able to activate the PI3K/AKT signaling pathway in cells, upregulating GPX4, and downregulating the expression levels of TRPM7 and ACSL4. Treatment with 2-aminoethoxydiphenyl borate (an inhibitor of TRPM7) could further strengthen the myocardial protective effects of MTH, whereas treatment with erastin (promoter of ferroptosis) and wortmannin (inhibitor of PI3K) led to the effective elimination of the myocardial protective effects of MTH. Compared with in the I/R group, the PI3K/AKT activation level and the expression levels of GPX4 were both significantly increased, whereas the expression levels of TRPM7 and ACSL4 were significantly decreased in the I/R + MTH group. Taken together, the results of the present study indicated that MTH may activate the PI3K/AKT signaling pathway to inhibit TRPM7 and suppress ferroptosis induced by MIRI.

## Introduction

Ischemic cardiomyopathy is one of the main causes of human mortality worldwide, accounting for ~30 million deaths annually (1-3). In addition, myocardial ischemia-reperfusion (I/R) injury (MIRI), which leads to the aggravation of disordered metabolism of myocardial cells during reperfusion following myocardial ischemia, thus causing myocardial ultrastructural damage, is one of the main causes of death in patients with ischemic heart disease (4,5). Previous studies have shown that MIRI is associated with numerous pathophysiological features, including the generation of oxygen free radicals, calcium overload, endothelial dysfunction, mitochondrial dysfunction, immune response, ferroptosis, myocardial cell apoptosis and autophagy (6-8). At present, ischemic preconditioning (IPC) and pharmacological preconditioning (PPC) offer the main means to improve MIRI in clinical practice (9); however, due

*Correspondence to:* Professor Jing Zhang or Professor Shuchun Yu, Department of Anesthesiology, The Second Affiliated Hospital of Nanchang University, 1 Minde Road, Donghu, Nanchang, Jiangxi 330006, P.R. China
E-mail: ndefy01467@ncu.edu.cn
E-mail: ndefy94004@ncu.edu.cn

*Contributed equally

*Key words:* mild therapeutic hypothermia, myocardial ischemia-reperfusion injury, transient receptor potential cation channel subfamily M member 7, PI3K/AKT signaling pathway

to the limited scope of their use, the identification of novel therapeutic methods and targets is necessary.

In 1997, Sessler (10) proposed the concept of mild perioperative hypothermia, highlighting that performing carotid endarterectomy and neurosurgery at a temperature of 33-35˚C could protect against cerebral ischemia. This was later confirmed by a large number of basic research studies and clinical trials (11-13). In addition, further studies have indicated that hypothermia can improve the ischemic injury of organs through a variety of different mechanisms (14,15). Notably, the PI3K/AKT signaling pathway has been shown to have an important role in organ reperfusion injury. A previous study showed that mild therapeutic hypothermia (MTH) combined with hydrogen sulfide treatment could reduce damage caused to the hippocampal neurons in rats via activating the PI3K/AKT signaling pathway, thereby improving cerebral I/R injury in rats (11). In addition, MTH has been shown to inhibit inflammatory reactions and reduce cell apoptosis through activating the PI3K/AKT signaling pathway, thereby improving liver I/R injury (16). MTH may also ameliorate MIRI (17). In another study, investigators revealed that MTH could effectively alleviate MIRI in a rabbit model (18). Mochizuki *et al* (19) demonstrated that MTH could improve MIRI in rats by activating the PI3K signaling pathway. In addition, certain studies have shown that MTH can reduce inflammatory reactions by inhibiting NLR family pyrin domain containing 3 inflammasomes, thereby inhibiting calcium channels and improving MIRI (17,20). However, the protective mechanism that accounts for the influence of MTH on MIRI has yet to be fully elucidated.

Transient receptor potential cation channel subfamily M member 7 (TRPM7) is a membrane protein with a dual structure of ion channel and protein kinase that, as a member of the TRP channel subfamily, is widely distributed in the heart, brain, lung, kidney, and other organs and tissues (21,22). TRPM7 is a non-selective cation channel with calcium-ion permeability that serves an important role in the I/R injury of various organs. Cerebral I/R injury has previously been studied in a rat model with overexpression of TRPM7, and the high expression of TRPM7 was shown to be inhibited by electroacupuncture through the PI3K pathway (23). Furthermore, inhibition of TRPM7 expression using small interfering RNA has been shown to effectively suppress the calcium overload induced by long-term oxygen-glucose deprivation, and to reduce the generation of reactive oxygen species (ROS), thereby promoting the survival of oxygen- and glucose-deprived neurons (24,25). The expression of TRPM7 has also been reported to be upregulated after renal ischemia (26). In addition, microRNA-9-5p has been reported to decrease the expression of TRPM7 by activating the PI3K/Akt pathway, thereby promoting both the migration and invasion of endothelial progenitor cells and angiogenesis (27). Notably, a recent study revealed that inhibition of TRPM7 expression may have a protective effect on the reperfusion injury of H9C2 cells, and that this could reduce the apoptotic rate of H9C2 cells (28).

Ferroptosis is a cell death process that results from the accumulation of iron-dependent lipid peroxides, which differs from traditional apoptosis and necrosis (29). The occurrence of ferroptosis is closely associated with various pathophysiological processes, including the blockade of cystine transport, the accumulation of reactive oxygen free radicals in cells, abnormal iron metabolism, accumulation of iron ions and lipid peroxidation (29,30). Of these processes, the accumulation of iron ions and lipid peroxidation are biochemically the most important (31). Numerous studies have demonstrated that ferroptosis has an important role in various types of cardiovascular disease, including heart failure, myocardial infarction and I/R injury (32-34). Lapatinib has been shown to enhance Adriamycin-induced oxidative stress and ferroptosis of cardiomyocytes through inhibiting the PI3K/AKT signaling pathway (35).

With the knowledge that TRPM7 exerts a key role in various cell death modalities (36), it was hypothesized that MTH could regulate the expression of TRPM7 through its action on the PI3K/AKT signaling pathway, thereby inhibiting ferroptosis induced by MIRI. In order to further clarify the underlying protective mechanism of MTH on MIRI, a rat model of MIRI was established, and the rats were treated with various drugs to explore the protective mechanism of MTH. Taken together, the findings of the present study offer several insights that may inform future strategies to relieve MIRI in animals or humans.

## Materials and methods

*Animals, chemical reagents and kits*. H9C2 cells, wortmannin (Wort) and erastin (Era) were purchased from Beyotime Institute of Biotechnology. A total of 86 healthy adult male Sprague-Dawley rats (age, 6-8 weeks; weight, 250-350 g) were purchased from Hunan SJA Laboratory Animal Co., Ltd. 2-Aminoethoxydiphenyl borate (2-APB) was obtained from Selleck Chemicals (cat. no. S6657). Antibodies against glutathione peroxidase 4 (GPX4; cat. no. 52455; Cell Signaling Technology, Inc.), acyl-CoA synthetase long chain family member 4 (ACSL4; cat. no. 22401-1-AP; Proteintech Group, Inc.), ferroptosis suppressor protein 1 (FSP1; cat. no. 20886-1-AP; Proteintech Group, Inc.), phosphorylated (p)-PI3K (cat. no. 17366; Cell Signaling Technology, Inc.), total (t)-PI3K (cat. no. 4249; Cell Signaling Technology, Inc.), p-AKT (cat. no. 4060; Cell Signaling Technology, Inc.), t-AKT (cat. no. 9272; Cell Signaling Technology, Inc.) and GAPDH (cat. no. AF0006; Beyotime Institute of Biotechnology) were used in the present study. ELISA kits for creatine kinase-MB (CK-MB; cat. no. H197-1-1), lactate dehydrogenase (LDH; cat. no. A020-1-2), cardiac troponin I (cTnI; cat. no. H149-2-1), malondialdehyde (MDA; cat. no. A003-1-1), total superoxide dismutase (SOD; cat. no. A001-1-1) and glutathione peroxidase (GSH-Px; cat. no. A005-1-2) were supplied by Nanjing Jiancheng Bioengineering Institute. In addition, the MTT cell viability assay kit was purchased from APeXBIO Technology LLC, and the LDH cytotoxicity assay kit and the cytoFLEX® Annexin V-FITC/PI apoptosis kit (cat. no. KGA108) were purchased from Nanjing KeyGen Biotech Co., Ltd.

*Cell culture and animal treatment*. H9C2 cells were resuscitated and subcultured. Subsequently, H9C2 cells in the exponential growth phase and in good growth condition were prepared into a single cell suspension in sugar-free and serum-free DMEM (Beyotime Institute of Biotechnology), with the cell concentration adjusted to $2.5x10^5$ cells/ml.

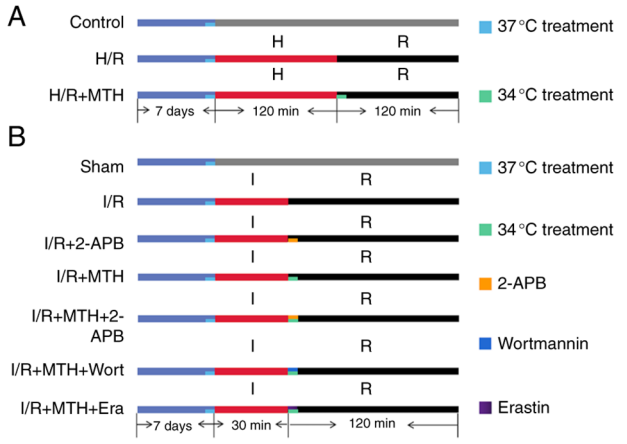


Figure 1. (A) Schematic diagram of the cell experimental protocol. (B) Schematic diagram of the animal experimental protocol. 2-APB, 2-aminoethoxydiphenyl borate; Era, erastin; H/R, hypoxia-reperfusion; I/R, ischemia-reperfusion; MTH, mild therapeutic hypothermia; Wort, wortmannin.

Subsequently, the cells were evenly inoculated into a 6-well plate (2 ml cell suspension/well), and the plate was incubated overnight at 37˚C in an atmosphere containing 5% $CO_2$ with saturated humidity. Cells were randomly divided into three groups (Fig. 1A): The control group (no treatments); the H/R group (subjected to hypoxia for 120 min, and then reoxygenation for 120 min at 37˚C); and the H/R + MTH group [MTH (34˚C) was induced during the 120-min reperfusion period].

Regarding the animal experiments, the Animal Experiment Ethics Committee of Nanchang University (Nanchang, China) provided full approval for the present study (approval no. NCULAE-20221121086). In addition, the present study followed the Animal Research: Reporting *In Vivo* Experiments Guidelines and the American Veterinary Medical Association Euthanasia Guidelines 2020 (37). A total of 86 healthy adult male Sprague-Dawley rats (weight, 250-350 g) were housed in cages, with each cage containing one rat, and were housed under standard conditions (humidity, 45-55%; temperature, 23-25˚C; 12-h light/dark cycle), with food and tap water given *ad libitum*. The cages were cleaned every 3 days. All rats were anesthetized prior to the experiment using 3% sodium pentobarbital (50 mg/kg), which was injected intraperitoneally with heparin. All rats were euthanized by an overdose of sodium pentobarbital (150 mg/kg), which was injected intraperitoneally at the end of the experiment.

For these experiments, the rats were randomly divided into seven groups (n=12/group) (Fig. 1B): The sham group (no treatments); the I/R group, wherein the rats were subjected to ischemia for 30 min, followed by reperfusion for 120 min at 37˚C; the I/R + 2-APB group, in which the TRPM7 inhibitor 2-APB (5 $\mu$M) was added during the reperfusion period; the I/R + MTH group, wherein MTH (at 34˚C) was induced during the 120-min reperfusion period; the I/R + MTH + 2-APB group, wherein 2-APB was administered combined with MTH (34˚C) during the reperfusion period; the I/R + MTH + Wort group, wherein the PI3K inhibitor Wort (1.5 $\mu$M) was added and MTH (34˚C) was implemented during the reperfusion period; and the I/R + MTH + Era group, wherein the ferroptosis promoter Era (10 $\mu$M) was added and MTH (34˚C) was implemented during the reperfusion period. All intervention drugs were added to modified Krebs-Henseleit (MKH) buffer during the first 15 min of reperfusion.

*Isolated heart model preparation and cell model establishment*. Firstly, the Langendorff model for I/R injury was constructed. Rats were first anesthetized using 3% sodium pentobarbital (50 mg/kg), and then heparin (1,000 IU/kg; n=12 rats) was injected intraperitoneally. After performing midline thoracotomy, the heart was excised within 1 min, and the aorta was cannulated for retrograde perfusion at a constant pressure of 80 mmHg using a Langendorff device with MKH buffer (120.0 mmol/l NaCl, 4.8 mmol/l KCl, 2.4 mmol/l $CaCl_2$, 25.0 mmol/l $NaHCO_3$, 1.21 mmol/l $KH_2PO_4$, 1.2 mmol/l $MgSO_4$ and 11.0 mmol/l glucose; pH, 7.40±0.05). The buffer was gassed continuously with 95% $O_2$ + 5% $CO_2$, and maintained at 37±0.2˚C or 34±0.2˚C with circulating water. The perfusate MKH buffer during the reperfusion phase needed to reach a temperature of 34˚C within 5 min in the MTH groups. The initial left ventricle end-diastolic pressure (LVEDP) was set to 10 mmHg using a latex balloon filled with bubble-free saline, and Med Lab 6.0 software (ZhongShiDiChuang Science and Technology Development Co., Ltd.) was used to record hemodynamic changes, including heart rate (HR), left ventricular systolic pressure (LVSP), LVEDP and ± dP/dt(max). Rats with frequent arrhythmia, refractory ventricular fibrillation, HR <180 beats/min or LVSP <75 mmHg were excluded from the study; a total of two rats excluded.

Secondly, the H/R cell model was constructed. The H9C2 cells were cultured in a low volume of substrate-free medium (serum-free and glucose-free) in an anaerobic Plexiglas chamber (Billups-Rothenberg, Inc.) containing 0.2% $O_2$, saturated with 95% $N_2$ and 5% $CO_2$ at 37˚C for 2 h. The volume of hypoxic medium used was the minimum volume required to coat the cellular monolayer for the prevention of cellular dehydration during the ischemic period. Simulated ischemia was followed by a simulated reperfusion period, during which the cells were exposed to normoxic culture medium at 37˚C for 2 h (Fig. 1A). For the hypothermia treatment, the ischemic and hypoxic cells were maintained in an incubator at 34˚C for 2 h in the reoxygenation stage. The control cells were cultured in growth medium at 37˚C in an atmosphere containing 5% $CO_2$ and 95% humidified air.

*Determination of myocardial infarct size*. After anesthetizing the rats, open chest surgery was performed and the rats were sacrificed by cervical dislocation before removing the heart. Subsequently, the hearts were immediately removed and a Langendorff model was established. After reperfusion for 2 h, the hearts were transferred to PBS solution (pH 7.4) maintained at 4˚C, and then frozen at -20˚C for 80 min. Each heart was cut into five cross-sections using a blade, and the sections were incubated in 1% 2,3,5-triphenyltetrazolium chloride (TTC) (prepared by dissolving 1 g TTC into 100 ml PBS; cat. no. TTC 0765; Ameresco, LLC) at 37˚C for 20 min. The hearts were fixed in 4% paraformaldehyde overnight at 37˚C. The myocardial infarct area changed to white, whereas the area at risk remained red. An Epson scanner (Seiko Epson Corporation) was used to scan each slice, and the myocardial infarct area, was calculated using Image Pro Plus software 6.0 (Media Cybernetics, Inc.).

*Hematoxylin and eosin (H&E) staining*. The myocardial tissue obtained from rats was fixed in 10% paraformaldehyde overnight at room temperature, followed by embedding in paraffin and cutting into 4-$\mu$m sections. These sections were subsequently dewaxed with xylene twice (5 min each) and hydrated with 95% ethanol. Subsequently, 0.5% hematoxylin solution was added for 10 min, and the sections were rinsed with tap water, differentiated with 1% HCl in ethanol for 10 sec, and finally stained with 5% eosin for 1-3 min; all steps were at room temperature. The stained sections were dehydrated with ethanol for 25 min, dewaxed with xylene, sealed and dried with neutral resin, and finally observed under a fluorescence microscope (magnification, x200; DMi8 DFC7000 T; Leica Microsystems, Inc.).

*Detection of cell viability and cytotoxicity*. Cell viability was measured using an MTT cell viability assay kit and cytotoxicity was measured using a LDH cytotoxicity assay kit. All steps were performed in strict accordance with the manufacturers' protocols.

*Cell apoptosis detection*. Cells were digested with 0.25% trypsin without EDTA. After the digestion was terminated, the cells were collected and centrifuged at 400 x g for 5 min at room temperature, after which the supernatant was removed and the cells were washed with PBS. The cells were then rinsed twice with PBS at 400 x g for 5 min at room temperature, and a cytoFLEX Annexin V-FITC/PI cell apoptosis detection kit was employed to assess the level of cell apoptosis. All of the steps were performed in strict accordance with the manufacturer's instructions. The samples were analyzed using a flow cytometer (BD Accuri C6 Plus; BD Biosciences) with FlowJo software (v10.6.2; FlowJo, LLC) according to the manufacturer's instructions.

*Determination of cardiac enzyme and oxidative stress indicator levels*. At the end of reperfusion in the Langendorff model, coronary effluent was collected for 3 min. Subsequently, the levels of cardiac muscle enzymes (CK-MB, LDH and c-TnI) were measured by ELISA. All steps were performed in strict accordance with the manufacturers' protocols. Furthermore, myocardial tissue was homogenized in RIPA buffer (cat. no. P0013C; Beyotime Institute of Biotechnology) containing benzamidine and benzoyl fluoride. The homogenate was then centrifuged at 15,000 x g for 25 min at 4˚C, and the supernatant was separated and stored at -80˚C. Oxidative stress markers (GSH-Px, MDA and SOD) in the supernatant were then measured by ELISA. All steps were performed strictly in accordance with the manufacturer's instructions.

*Western blot analysis*. Total proteins were extracted from cell samples or homogenized hearts using a kit (Total Protein Extraction Kit; cat. no. P1250; Applygen Technologies, Inc.) according to the manufacturer's instructions. The clarified supernatant was separated from the sample by centrifugation at 12,000 x g for 5 min using an MGL-16M desktop high-speed freezing centrifuge at 4˚C. Subsequently, a BCA reagent kit (cat. no. 23227; Thermo Fisher Scientific, Inc.) was used to quantify the protein concentration, according to the manufacturer's instructions. Proteins (20 $\mu$g/lane) were then separated by SDS-PAGE on 8% gels and were transferred to polyvinylidene fluoride (PVDF) membranes. Subsequently, the PVDF membranes were blocked in 10% non-fat milk for 2 h at room temperature, prior to incubation with primary antibodies against TRPM7 (1:500; cat. no. ACC-047; Alomone Labs), t-PI3K (1:1,000), p-PI3K (1:1,000), p-AKT (1:1,000), t-AKT (1:1,000), GPX4 (1:1,000), ASCL4 (1:2,000) and FSP1 (1:1,000) at 4˚C overnight, followed by incubation with horseradish peroxidase-conjugated anti-rabbit IgG (cat. no. 7074S; Cell Signaling Technology, Inc.) or anti-mouse IgG (cat. no. 7076S; Cell Signaling Technology, Inc.) secondary antibodies (1:700, diluted in 5% non-fat milk) at room temperature for 2 h. The same membrane was probed with anti-GAPDH as a control for normalization of the levels of the proteins of interest. Protein bands were detected by chemiluminescence (cat. no. P90720; MilliporeSigma) and the images were semi-quantified using ImageJ version 1.51 software (National Institutes of Health).

*Statistical analysis*. All measurements were performed by two researchers in a double-blinded manner. Data are shown as the mean ± standard deviation, based on a minimum of three independent replicates. One-way analysis of variance was employed, followed by Tukey's post hoc test for multiple comparisons to assess the differences across multiple groups and to evaluate the impact of treatments on data derived from animal and cell studies. Statistical analysis was performed using GraphPad Prism software (version 9.5; Dotmatics). $P<0.05$ was considered to indicate a statistically significant difference.

## Results

*MTH improves cell viability, and inhibits the release of LDH and cardiomyocyte apoptosis induced by H/R*. In our previous study (19), it was revealed that MTH (set at 34˚C) was able to effectively improve MIRI. Therefore, based on this previous research, the present study aimed to further investigate the specific underlying protective mechanism. In the present study, it was revealed that cell viability was reduced, whereas the release of LDH and the level of apoptosis were increased in the H/R group compared with those in the control group (Fig. 2). However, implementing conditions of MTH reversed this process through increasing cell viability, and reducing the release of LDH and cardiac myocyte apoptosis (Fig. 2), thus suggesting that MTH nay exert a certain myocardial protective effect.

*MTH exerts its protective effect on myocardial cells by inhibiting H/R-mediated ferroptosis through the PI3K/AKT/TRPM7 signaling axis*. In order to further clarify the myocardial protective mechanism of MTH, a hypothesis was proposed based on previous research (8), and western blot analysis was performed to detect the corresponding indicators. First, the expression levels of p-PI3K, p-AKT and TRPM7 were measured in each group of cells, which revealed that the phosphorylation levels of PI3K and AKT in the H/R group were between one-half and one-third the levels of those in the control group, and the expression levels of TRPM7 were 3-4 times higher compared with those in the control group (Fig. 3A, D, F and H). By contrast, the phosphorylation levels of PI3K and AKT in the H/R + MTH group were higher compared with those in the H/R group, whereas the expression levels of TRPM7 were reduced.

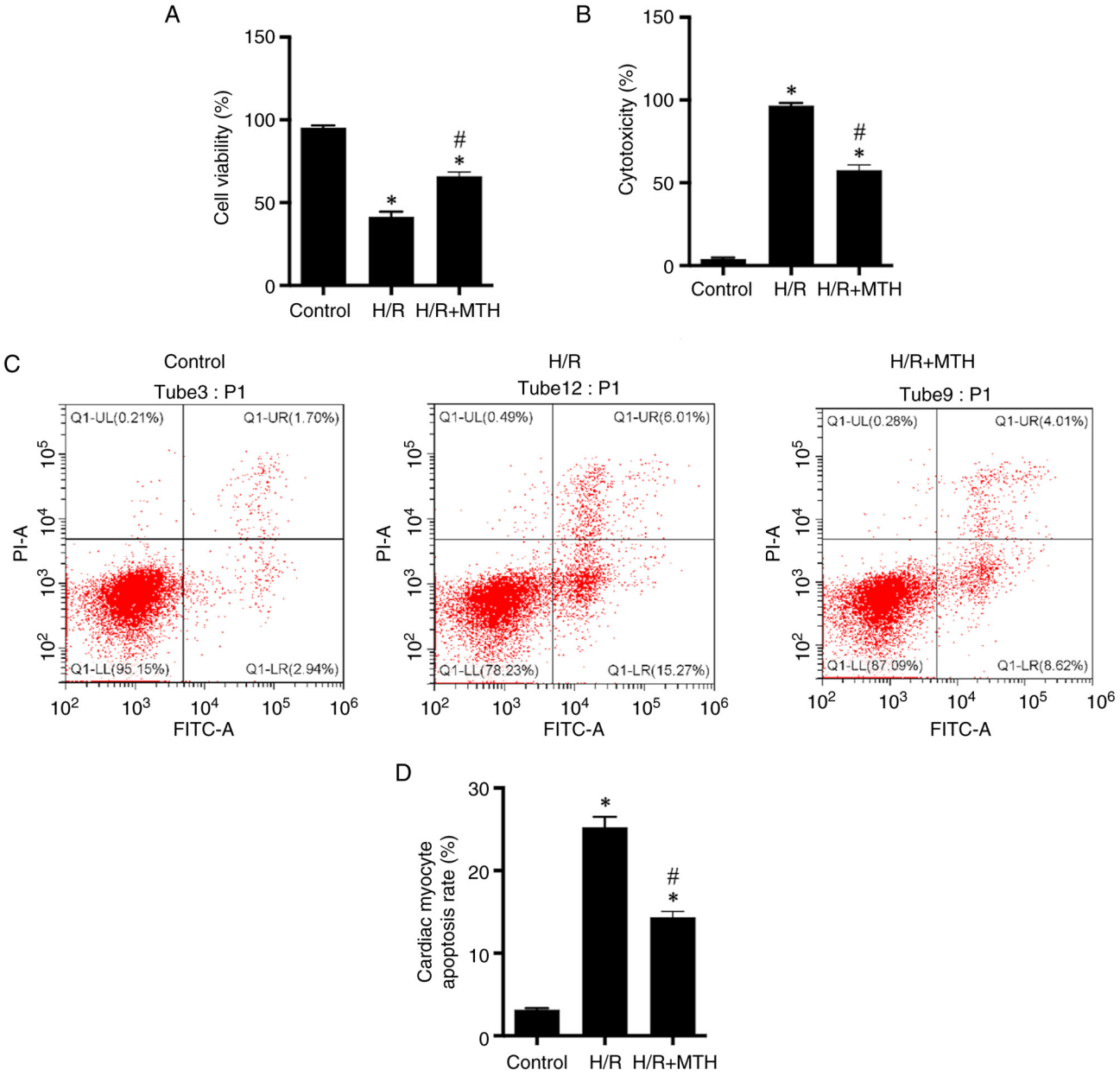


Figure 2. Cardiomyocyte viability, cytotoxicity and apoptosis. (A) Viability of H9C2 cells was examined using a MTT cell viability assay kit. (B) Cytotoxicity in H9C2 cells was examined using a lactate dehydrogenase cytotoxicity assay kit. (C) Flow cytometric analysis of the levels of H9C2 cell apoptosis. (D) Statistical analysis of apoptosis rate. *P<0.05 vs. control group; #P<0.05 vs. H/R group. H/R, hypoxia-reperfusion; MTH, mild therapeutic hypothermia.

Subsequently, the expression levels of GPX4, ACSL4 and FSP1 in the H9C2 cells were examined in each group (Fig. 3B, C, E, G and I). The expression levels of GPX4 were decreased and the expression levels of ACSL4 were increased in the H/R group compared with those in the control group. By contrast, MTH treatment reversed this process; ACSL4 expression levels were significantly decreased, whereas GPX4 expression levels were significantly increased compared with those in the H/R group. Furthermore, the expression levels of FSP1 were significantly decreased in the H/R group, whereas they were significantly higher in the MTH group compared with those in the H/R group. Taken together, these data suggested that MTH may reduce H/R-mediated ferroptosis through the PI3K/AKT/TRPM7 signaling axis.

*MTH reduces the myocardial infarct area and improves hemodynamic performance following I/R injury in rats*. To determine whether MTH exerts a protective effect on MIRI, analysis of the myocardial infarct area and the hemodynamics of rats was performed for each group. Compared with in the I/R group, the myocardial infarct area was significantly reduced in all rats with I/R injury subjected to MTH, except in the MTH + Wort/Era groups (Fig. 4), which confirmed that MTH could protect against myocardial injury caused by I/R. In addition, it was revealed that the ferroptosis promoter Era, the PI3K inhibitor Wort and the TRPM7 inhibitor 2-APB could affect the protective effect of MTH on MIRI. Compared with in the I/R + MTH group, the myocardial infarct area of the I/R + MTH + 2-APB group was significantly reduced, whereas the area was significantly increased in the I/R + MTH + Wort

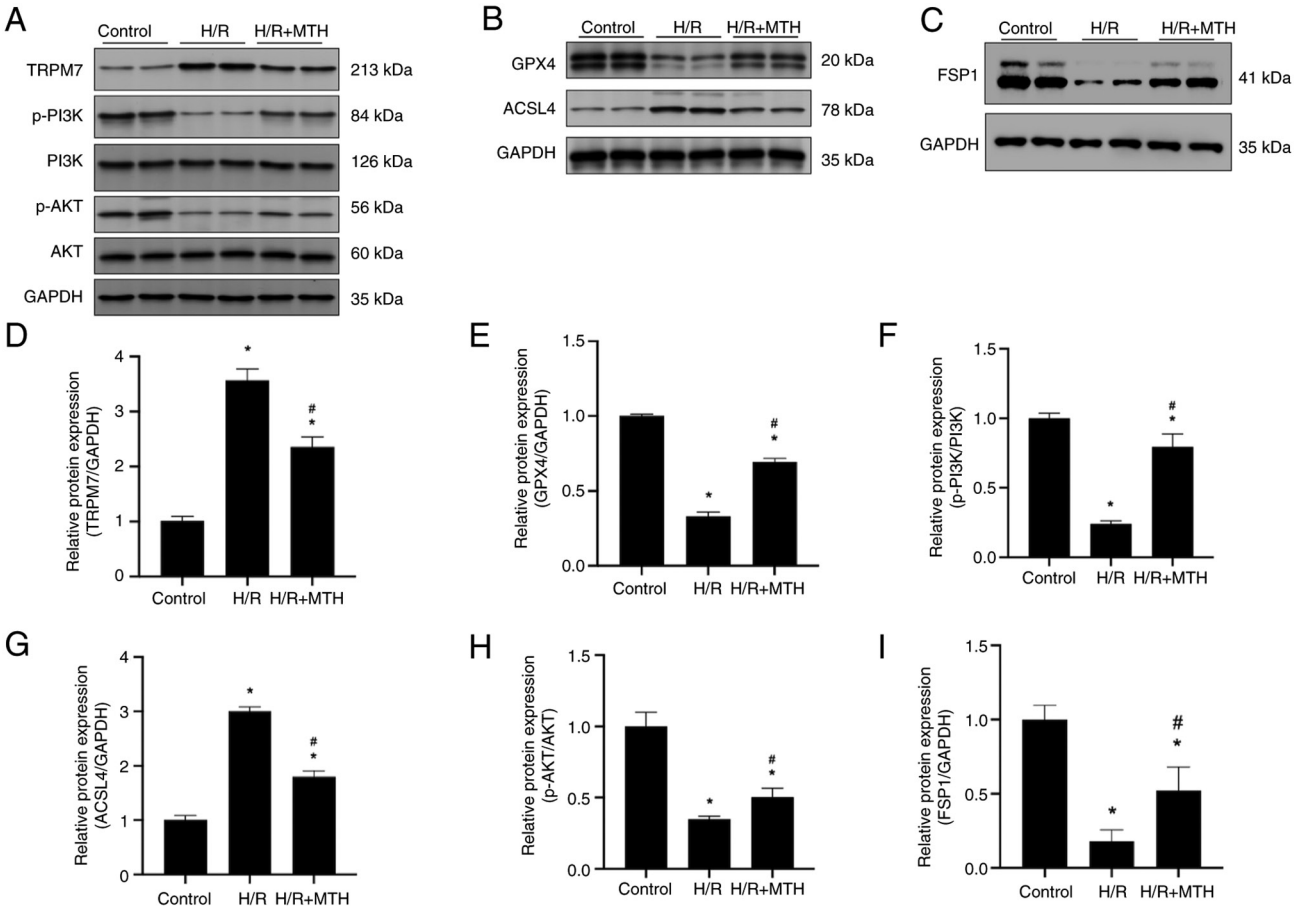


Figure 3. PI3K/AKT phosphorylation, TRPM7 expression levels and the expression level of ferroptosis-associated proteins in cells. Western blot analyses of (A) TRPM7, p-PI3K, PI3K, p-AKT and AKT; (B) GPX4 and ACSL4; and (C) FSP1. The expression levels of (D) TRPM7, (E) GPX4, (F) p-PI3K, (G) ACSL4, (H) p-AKT and (I) FSP1 are shown. $^{*}$P<0.05 vs. control group; $^{\#}$P<0.05 vs. H/R group. ACSL4, acyl-CoA synthetase long chain family member 4; FSP1, ferroptosis suppressor protein 1; GPX4, glutathione peroxidase 4; H/R, hypoxia-reperfusion; MTH, mild therapeutic hypothermia; p-, phosphorylated; TRPM7, transient receptor potential cation channel subfamily M member 7.

and I/R + MTH + Era groups, suggesting that I/R could induce ferroptosis of myocardial cells. Moreover, the inhibitory effect of MTH on myocardial cell ferroptosis induced by I/R may be associated with the expression levels of p-PI3K and TRPM7.

In addition, the hemodynamics of all groups of rats were recorded to further elucidate the effects of MTH and various drugs on myocardial infarction (Table I). The results showed no significant differences in the HR or heart rate pressure product values among all of the groups at baseline. However, compared with in the sham group, significant changes in HR, LVEDP, LVSP and ± dP/dt(max) were observed in other groups at 30, 60, 80 and 120 min. As expected, MTH treatment led to significant reductions in the HR, LVSP and ± dP/dt(max) values, whereas the LVEDP values were increased. The PI3K inhibitor Wort and the ferroptosis promoter Era were able to inhibit the effects of MTH, whereas treatment with the TRPM7 inhibitor 2-APB was found to enhance the effect of MTH, suggesting that MTH exerts an influence on the expression levels of PI3K and TRPM7, and on the occurrence of ferroptosis.

*MTH alleviates MIRI in rats*. To further verify the protective effect of MTH on MIRI, the myocardial tissue of rats was stained with H&E, and the results obtained showed that, compared with in the control group, the myocardial tissue of rats in the I/R group exhibited clear pathological changes. Specifically, the myocardial cells were disordered; some myocardial cells were seen to be broken and dissolved; edema and some degeneration were observed; and the cell gap was notably widened (Fig. 5A). However, the negative pathological changes observed in the myocardial tissue of I/R model rats were found to be improved following treatment with MTH or 2-APB, and the myocardial cells were arranged neatly. Notably, compared with in the I/R + MTH group, the pathological changes observed in the myocardial tissue of the I/R model rats treated with MTH + 2-APB were further improved; myocardial cells and clear morphological structures were both found to be well-arranged, and myocardial cell edema and cell degeneration were suppressed, thus suggesting that 2-APB may enhance the effect of MTH through inhibiting the expression of TRPM7. However, the I/R model rats in the MTH + Wort and MTH + Era treatment groups exhibited obvious pathological changes, which were not notably different from those observed in the I/R group.

In addition, the concentrations of CK-MB, LDH and cTnI were measured by ELISA. Compared with those in the sham group, the levels of CK-MB, LDH and cTnI in the I/R group rats were significantly increased, whereas the levels of CK-MB, LDH and cTnI in the rats treated with MTH or

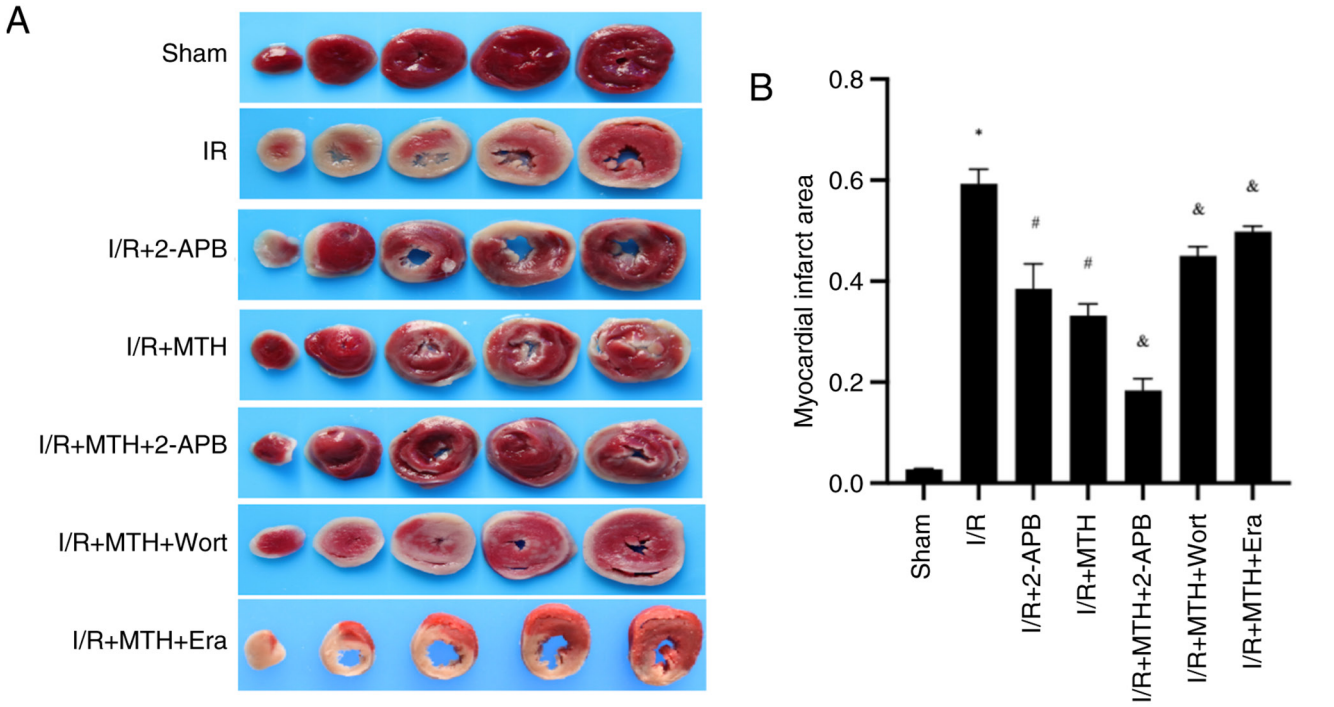


Figure 4. TTC staining results of myocardial infarction. (A) Myocardial sections following TTC staining. (B) Semi-quantitative analysis of the TTC staining results of myocardial infarction. *P<0.05 vs. sham group; #P<0.05 vs. I/R group; &P<0.05 vs. I/R + MTH group. 2-APB, 2-aminoethoxydiphenyl borate; Era, erastin; I/R, ischemia-reperfusion; MTH, mild therapeutic hypothermia; TTC, 2,3,5-triphenyltetrazolium chloride; Wort, wortmannin.

2-APB were decreased (Fig. 5B-D). In addition, compared with in the I/R + MTH group, the levels of CK-MB, LDH and cTnI were significantly decreased in the I/R + MTH + 2-APB group, whereas they were increased in the I/R + MTH + Wort and I/R + MTH + Era groups. Taken together, these results suggested that MTH could improve MIRI, and that the protective effect of MTH was affected by the expression levels of PI3K and TRPM7, and by whether ferroptosis occurred.

*MTH is able to reduce MIRI in rats through activating the PI3K/AKT signaling pathway*. Subsequently, the activation levels of PI3K and AKT were detected in the rats (Fig. 6A, C and D). Compared with in the sham group, the phosphorylation levels of PI3K and AKT in the I/R group rats were significantly decreased; however, a higher phosphorylation level of PI3K and AKT was observed in the I/R + MTH group compared with that in the I/R group. Furthermore, the phosphorylation levels of PI3K and AKT were significantly decreased following treatment with Wort, compared with those in the I/R + MTH group. Notably, no significant differences in the phosphorylation levels of PI3K and AKT were observed between the I/R and I/R + 2-APB groups, between the I/R + MTH and I/R + MTH + 2-APB groups, or between the I/R + MTH and I/R + MTH + Era groups. Collectively, these data revealed that neither Era nor 2-APB affected the phosphorylation levels of PI3K and AKT, suggesting that MTH is able to regulate the expression of TRPM7 and the occurrence of ferroptosis through activating the PI3K/AKT signaling pathway, thereby protecting MIRI.

*MTH improves MIRI by activating the PI3K/AKT signaling pathway to inhibit the expression of TRPM7*. To further verify the hypothesis, the expression levels of TRPM7 were determined (Fig. 6A and B). Compared with in the sham group, the expression levels of TRPM7 in the I/R group were significantly increased, whereas the expression levels of TRPM7 were inhibited in the I/R + MTH group, suggesting that MTH treatment could downregulate the expression of TRPM7. Moreover, compared with in the I/R + MTH group, the expression levels of TRPM7 in the I/R + MTH + 2-APB group were significantly decreased, and a higher expression of TRPM7 was detected in the I/R + MTH + Wort group. These findings suggested that, under MTH conditions, the expression of TRPM7 may be inhibited through activating the PI3K/AKT signaling pathway, and that 2-APB may enhance the inhibitory effect of MTH. No significant difference in the expression levels of TRPM7 was observed between the I/R + MTH and I/R + MTH + Era groups, revealing that Era did not affect the expression levels of TRPM7.

*MTH is able to inhibit ferroptosis induced by MIRI through the PI3K/AKT signaling pathway*. To further clarify the association between ferroptosis and the PI3K/AKT signaling pathway, the expression levels of GPX4 and ACSL4 were examined in the rats in each group (Fig. 6E-G). The expression levels of GPX4 in the I/R group were significantly decreased compared with those in the sham group. Following MTH or 2-APB treatment, the expression levels of GPX4 were increased, suggesting that MTH and 2-APB could inhibit the occurrence of ferroptosis. Moreover, compared with in the I/R + MTH group, the expression levels of GPX4 in the I/R + MTH + 2-APB group were significantly increased, and the expression levels of GPX4 in the I/R + MTH + Wort group were decreased by 50%. These findings suggested that 2-APB may enhance the protective

Table I. Detection of hemodynamic parameters.

| Hemodynamic assessment | Reperfusion | | | | |
|---|---|---|---|---|---|
| | Baseline (T0) | 30 min (T1) | 60 min (T2) | 90 min (T3) | 120 min (T4) |
| HR, bpm | | | | | |
| Sham group | 302.66±18.20 | 287.10±5.00 | 286.59±8.26 | 281.30±11.43 | 280.26±8.41 |
| I/R group | 288.64±6.02 | 218.45±22.52[a] | 205.43±5.67[a] | 180.41±5.16[a] | 150.04±4.75[a] |
| I/R + 2-APB group | 299.98±4.75 | 255.04±4.96[a,b] | 219.27±15.23[a,b] | 225.37±15.39[a,b] | 213.42±8.19[a,b] |
| I/R + MTH group | 297.76±5.69 | 250.07±7.05[a,b] | 277.42±14.40[a,b] | 209.66±6.93[a,b] | 196.74±9.57[a,b] |
| I/R + MTH + 2-APB group | 300.47±6.65 | 273.91±3.19 | 255.71±14.69[a] | 251.91±8.83[a] | 242.83±5.71[a] |
| I/R + MTH + Wort group | 293.66±8.27 | 208.10±5.99[a,c] | 210.96±11.88[a,c] | 186.37±8.40[a] | 167.74±3.87[a,c] |
| I/R + MTH + Era group | 296.66±6.51 | 204.67±4.16[a,c] | 208.04±8.15[a,c] | 189.74±9.75[a] | 165.69±2.31[a,c] |
| LVEDP, mmHg | | | | | |
| Sham group | 7.18±0.39 | 6.89±0.59 | 6.06±0.29 | 6.11±0.52 | 5.67±0.46 |
| I/R group | 6.85±0.59 | 33.79±2.60[a] | 39.85±1.10[a] | 45.12±1.63[a] | 48.91±2.44[a] |
| I/R + 2-APB group | 7.29±0.42 | 19.12±0.33[a] | 19.68±0.83[a,b] | 22.03±0.24[a,b] | 27.10±0.25[a,b] |
| I/R + MTH group | 7.27±0.68 | 19.87±0.36[a] | 21.57±0.86[a,b] | 25.14±0.60[a,b] | 29.98±0.11[a,b] |
| I/R + MTH + 2-APB group | 6.94±0.86 | 10.14±0.69[a] | 11.12±0.59[a] | 14.06±0.55[a] | 17.01±0.29[a] |
| I/R + MTH + Wort group | 6.65±0.45 | 29.09±1.46[a] | 33.56±0.41[a,c] | 41.87±1.75[a,c] | 47.10±0.52[a,c] |
| I/R + MTH + Era group | 7.33±0.48 | 29.39±1.10[a] | 34.40±0.67[a,c] | 43.58±1.29[a,c] | 46.52±0.98[a,c] |
| LVSP, mmHg | | | | | |
| Sham group | 103.81±7.09 | 95.15±8.98 | 91.16±9.93 | 93.76±11.92[a] | 88.05±3.35[a] |
| I/R group | 103.15±4.98 | 62.02±8.12[a] | 50.08±4.72[a] | 41.08±3.82[a] | 28.63±5.42[a] |
| I/R + 2-APB group | 96.37±7.12 | 84.30±1.23[a] | 69.61±4.89[a] | 62.52±3.42[a] | 67.51±2.34[a] |
| I/R + MTH group | 103.27±8.58 | 81.33±2.73[a] | 66.85±2.44[a] | 57.34±1.61[a] | 56.03±4.07[a] |
| I/R + MTH + 2-APB group | 99.73±2.61 | 88.92±1.41 | 79.74±5.37[a] | 76.63±4.89[a] | 69.57±2.87[a] |
| I/R + MTH + Wort group | 63.83±1.00 | 63.83±1.00[a] | 57.30±1.67[a] | 46.18±2.76[a] | 32.26±8.13[a] |
| I/R + MTH + Era group | 64.63±0.88 | 64.63±0.88[a] | 56.88±1.08[a] | 45.87±2.83[a] | 31.23±9.06[a] |
| +dP/dt(max), mmHg/sec | | | | | |
| Sham group | 2,703.57±166.22 | 2,605.05±128.14 | 2,660.96±160.54 | 2,609.83±176.35 | 2,515.96±168.90 |
| I/R group | 2,891.98±101.97 | 1,724.36±179.88[a] | 1,538.13±106.34[a,b] | 1,205.16±246.80[a,b] | 851.32±60.81[a,b] |
| I/R + 2-APB group | 2,862.30±81.92 | 2,518.11±162.52[b] | 2,150.19±131.84[a,b] | 2,033.59±108.93[a,b] | 1,896.02±189.31[a,b] |
| I/R + MTH group | 2,773.18±156.28 | 2,393.79±78.29[b] | 2,023.00±66.09[a] | 1,900.44±86.25[a] | 1,830.33±181.71[a] |
| I/R + MTH + 2-APB group | 2,918.62±118.30 | 2,573.60±80.10 | 2,354.58±78.47[a] | 2,367.53±83.92 | 2,518.84±122.80[a] |
| I/R + MTH + Wort group | 2,759.03±253.44 | 1,810.25±89.80[a,c] | 1,475.58±83.63[a,c] | 1,192.34±86.02[a,c] | 979.77±98.81[a,c] |
| I/R + MTH + Era group | 2,714.76±150.42 | 1,657.27±341.90[a,c] | 1,481.72±92.60[a,c] | 1,210.00±120.82[a,c] | 932.13±112.38[a,c] |
| -dP/dt(max), mmHg/sec | | | | | |

Table I. Continued.

| Hemodynamic assessment | Reperfusion | | | | |
|---|---|---|---|---|---|
| | Baseline (T0) | 30 min (T1) | 60 min (T2) | 90 min (T3) | 120 min (T4) |
| Sham group | -2,785.34±133.79 | -2,528.84±187.12 | -2,589.51±96.94 | -2,514.40±292.89 | -2,696.33±181.73 |
| I/R group | -2,750.15±86.02 | -1,758.31±114.46[a] | -1,514.12±77.14[a] | -1,227.65±84.21[a] | -830.36±64.71[a] |
| I/R + 2-APB group | -2,867.99±163.77 | -2,566.42±86.04[b] | -2,066.89±54.34[a,b] | -2,043.36±107.16[a,b] | -1,905.83±170.75[a,b] |
| I/R + MTH group | -2,757.58±173.15 | -2,439.87±152.32[b] | -1,927.35±161.08[a,b] | -1,908.28±133.05[a,b] | -1,863.66±68.43[a,b] |
| I/R + MTH + 2-APB group | -2,882.22±112.48 | -2,598.29±65.88 | -2,413.16±96.44 | -2,322.91±84.80 | -2,138.46±45.25[a] |
| I/R + MTH + Wort group | -2,733.51±253.68 | -1,863.77±79.23[a,c] | -1,581.44±75.12[a,c] | -1,184.09±62.19[a,c] | -954.36±112.69[a,c] |
| I/R + MTH + Era group | -2,660.97±245.14 | -1,669.67±156.29[a,c] | -1,496.65±168.57[a,c] | -1,196.06±111.58[a,c] | -949.58±104.47[a,c] |

[a]P<0.05 vs. sham group; [b]P<0.05 vs. I/R group; [c]P<0.05 vs. I/R + MTH group. 2-APB, 2-aminoethoxydiphenyl borate; Era, erastin; HR, heart rate; I/R, ischemia-reperfusion; LVSP, left ventricular peak pressure; LVEDP, left ventricular end diastolic pressure; MTH, mild therapeutic hypothermia; Wort, wortmannin.

effect of MTH through inhibiting TRPM7, whereas Wort may damage the protective effect of MTH through inhibiting the PI3K/AKT signaling pathway. These findings were consistent with the aforementioned experimental results obtained from investigating the myocardial infarct area and improvements in hemodynamic performance following I/R injury in rats.

The expression changes of ACSL4 in each group were found to be the opposite of those reported for GPX4. Compared with in the sham group, the expression levels of ACSL4 in the I/R group were significantly increased. Following treatment with MTH or 2-APB, the expression levels of ACSL4 were decreased. Moreover, a greater decrease in the expression levels of ACSL4 was observed in the I/R + MTH + 2-APB group when compared with the I/R + MTH group, whereas the change in expression of ACSL4 showed an opposite trend in the I/R + MTH + Wort and I/R + MTH + Era groups. These findings suggested that MTH may be able to inhibit the expression of TRPM7 through activating the PI3K/AKT signaling pathway, which subsequently inhibits the occurrence of ferroptosis, thereby eventually producing a protective effect on MIRI. In addition, the levels of the oxidative stress markers (GSH-Px, SOD and MDA) were further tested in the myocardial tissue of each group of rats (Fig. 6H-J). These experiments revealed that the levels of GSH-Px and SOD in the MTH group were significantly higher compared with those in the I/R group, whereas the levels of MDA were significantly lower compared with those in the I/R group, further confirming that MTH may alleviate ferroptosis induced by MIRI by inhibiting oxidative stress.

## Discussion

MIRI, which may arise after myocardial ischemia, cardiac surgery or circulatory arrest, contributes to adverse cardiovascular outcomes. During this process, the lack of blood flow to the heart leads to an imbalance between oxygen demand and supply and, in turn, damage to the cardiac tissue (37). To date, a number of studies have identified several mechanisms involved in MIRI, including ferroptosis, calcium overload, inflammation and oxidative stress (38-40). Myocardial ischemia leads to the abnormal functioning of ion channels in cardiomyocytes, increasing intracellular calcium concentration. Following blood reperfusion, the calpain system is rapidly activated, thereby promoting cardiomyocyte apoptosis (38,39). At the same time, following myocardial infarction and reperfusion, MIRI promotes the increase of iron ions in the myocardium and induces ferroptosis (40). IPC and PPC represent the main treatments for MIRI; however, their therapeutic effects remain unsatisfactory.

Numerous studies have suggested that MTH is able to effectively improve MIRI (41-43), and the results of the present study were consistent with these previous findings. In the present study, it was observed that MTH improved cell viability, inhibited LDH release and reduced the rate of cardiac myocyte apoptosis. In addition, the results revealed that the myocardial infarct area in all rats with I/R injury under MTH conditions was significantly reduced compared with that in the I/R group; however, Era and Wort could effectively abolish the cardioprotective effect of MTH. Furthermore, subjecting the rats to MTH conditions led to a significant reduction in

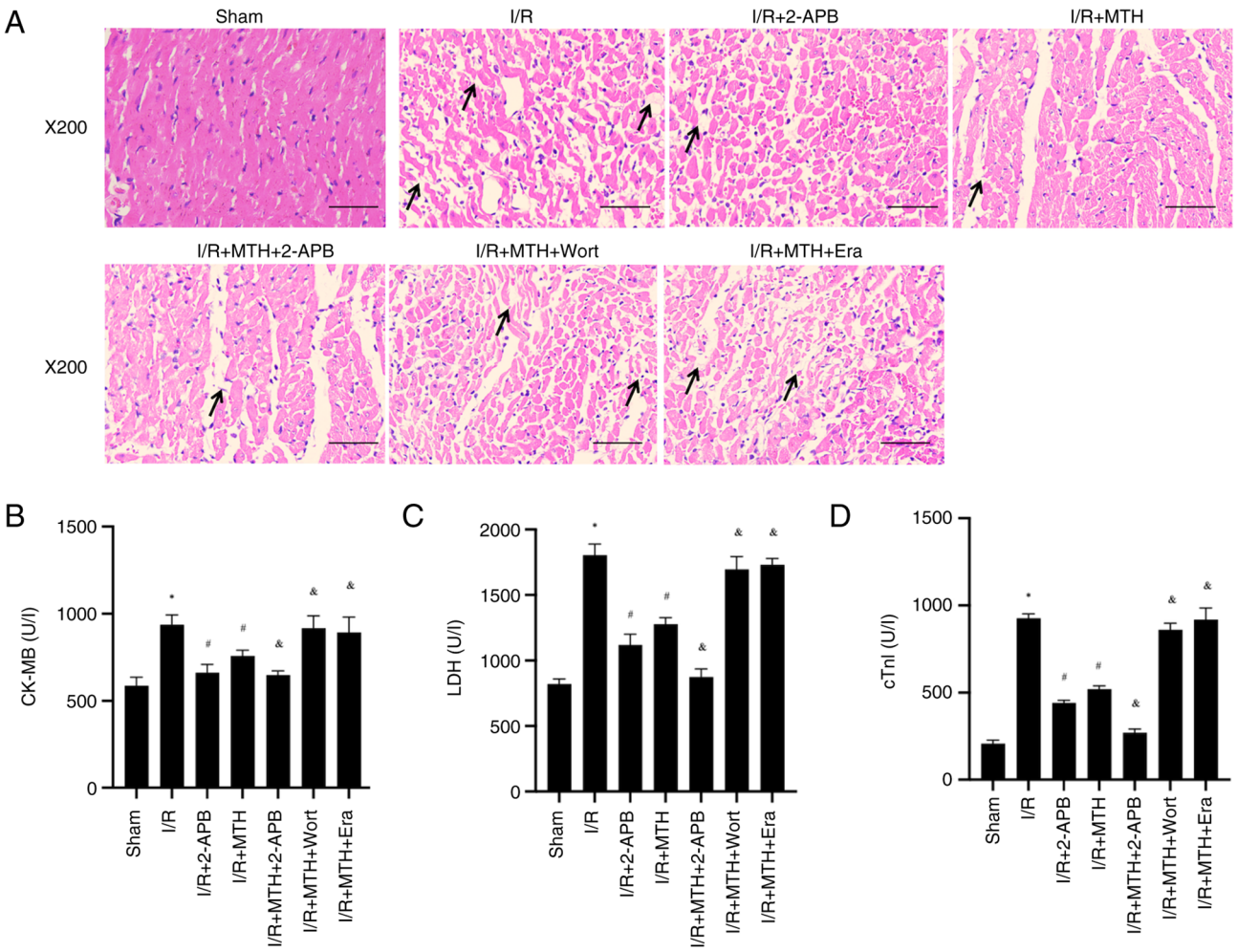


Figure 5. Pathological changes of myocardial tissue and levels of myocardial enzymes. (A) Hematoxylin and eosin staining, arrows indicate the location of myocardial fiber rupture or dissolution. Levels of (B) CK-MB, (C) LDH and (D) cTnI. *P<0.05 vs. sham group; #P<0.05 vs. I/R group; &P<0.05 vs. I/R + MTH group. 2-APB, 2-aminoethoxydiphenyl borate; CK-MB, creatine kinase-MB; cTnI, cardiac troponin I; Era, erastin; I/R, ischemia-reperfusion; LDH, lactate dehydrogenase; MTH, mild therapeutic hypothermia; Wort, wortmannin.

the HR, LVSP and ± dP/dt(max) values, and an increase in the LVEDP of rats with I/R injury.

Several studies have indicated that MTH exerts a protective effect on various types of cardiovascular injury. For example, MTH has been shown to inhibit both inflammatory reactions and cardiomyocyte apoptosis, thereby effectively improving MIRI in septic rats (44). Moreover, clinical trials showed that MTH effectively led to an improvement in the prognosis of patients with out-of-hospital cardiac arrest (45-47). Furthermore, MTH may exert a protective effect on acute myocardial infarction. Notably, MTH (at 34˚C) has been shown to effectively improve MIRI (17) and the findings of the present study lend support to this previous study. In the present study, clear pathological changes were identified in the myocardial tissue of I/R rats, with disorganized myocardial cell arrangement, partial myocardial cell fracture and lysis, myocardial cell edema and degeneration, and a notable widening of cell gaps. However, the disruptive pathological changes observed in the myocardial tissue of I/R model rats were markedly ameliorated following treatment with MTH or 2-APB, and the myocardial cells were shown to be neatly arranged. Compared with those in the I/R group, the levels of CK-MB, LDH and cTnI also exhibited significant decreases in the rats treated with MTH or 2-APB. Similarly, it was confirmed that implementing MTH conditions led to improvements in the H/R-induced decrease in cell viability, a reduction in the rate of LDH release and a reduction in the apoptotic rate of cardiac myocytes *in vitro*.

PI3K/AKT is an important signaling pathway in organisms that comprises PI3K and the downstream molecule, AKT (48). The PI3K/AKT pathway is activated via the receptor tyrosine kinase. Tyrosine residues are subsequently phosphorylated, providing binding sites for PI3K translocation to the cell membrane, thereby transducing signals to various extracellular matrices and cytokines (48). The pathway serves important roles in numerous cellular processes, including adhesion, proliferation, migration, metabolism, invasion and survival (49). In addition, numerous studies have shown that the PI3K/AKT signaling pathway participates in the occurrence and development of various types of cardiovascular disease (50). Notably, resveratrol has been shown to reduce myocardial cell apoptosis and mitochondrial oxidative damage caused by MIRI by activating PI3K/AKT (51,52), suggesting that activation of the PI3K/AKT signaling pathway may protect

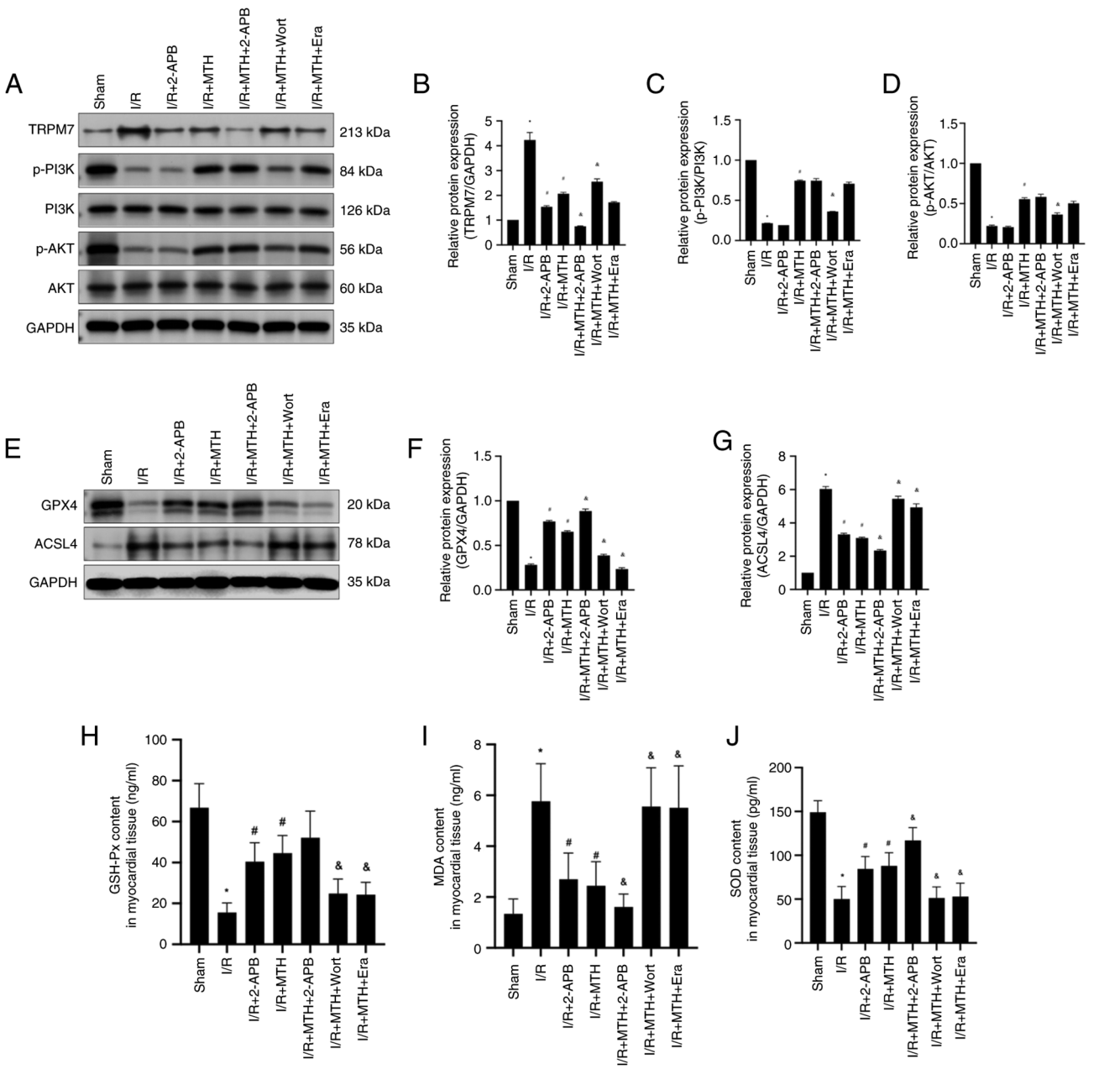


Figure 6. PI3K/AKT phosphorylation, TRPM7 expression levels and the expression level of ferroptosis-associated proteins. (A) Western blot analysis of TRPM7, p-PI3K, PI3K, p-AKT and AKT. Expression levels of (B) TRPM7, (C) p-PI3K and (D) p-AKT. (E) Western blot analysis of GPX4 and ACSL4. Expression levels of (F) GPX4 and (G) ACSL4. Levels of the oxidative stress indicators (H) GSH-Px, (I) MDA and (J) SOD. *P<0.05 vs. sham group; #P<0.05 vs. I/R group; &P<0.05 vs. I/R + MTH group. 2-APB, 2-aminoethoxydiphenyl borate; ACSL4, acyl-CoA synthetase long chain family member 4; Era, erastin; GPX4, glutathione peroxidase 4; GSH-Px, glutathione peroxidase; I/R, ischemia-reperfusion; MDA, malondialdehyde; MTH, mild therapeutic hypothermia; p-, phosphorylated; SOD, superoxide dismutase; TRPM7, transient receptor potential cation channel subfamily M member 7; Wort, wortmannin.

against MIRI. Furthermore, MTH has been shown to activate the PI3K signaling pathway to protect the myocardium from I/R injury (19). In addition, as an inhibitor of PI3K, a previous study demonstrated that 1 $\mu$M Wort could effectively inhibit the protective effect of MTH on MIRI (17). Therefore, the same concentration of Wort was chosen for the experiments in the present study. Notably, the PI3K signaling pathway is able to improve I/R injury through regulating the expression levels of TRPM7 (21). The present study revealed that MTH affected the physiological levels of PI3K and AKT in cells *in vitro*. Subsequently, the animal intervention experiments showed that, compared with in the I/R group, the phosphorylation levels of PI3K and AKT were significantly increased in the I/R + MTH group; however, no significant differences in the PI3K or AKT phosphorylation levels were observed between the I/R + MTH and the I/R + MTH + 2-APB groups. These results provided further evidence to indicate that the expression levels of TRPM7 are regulated by the PI3K/AKT signaling pathway, thereby providing further evidence for our hypothesis.

TRPM7 is a protein with a dual structure consisting of a cationic channel and a serine/threonine protein kinase, which has been reported to be temperature-sensitive (49); 2-APB is as an inhibitor of TRPM7. A previous study showed that 5 $\mu$M 2-APB was able to effectively inhibit

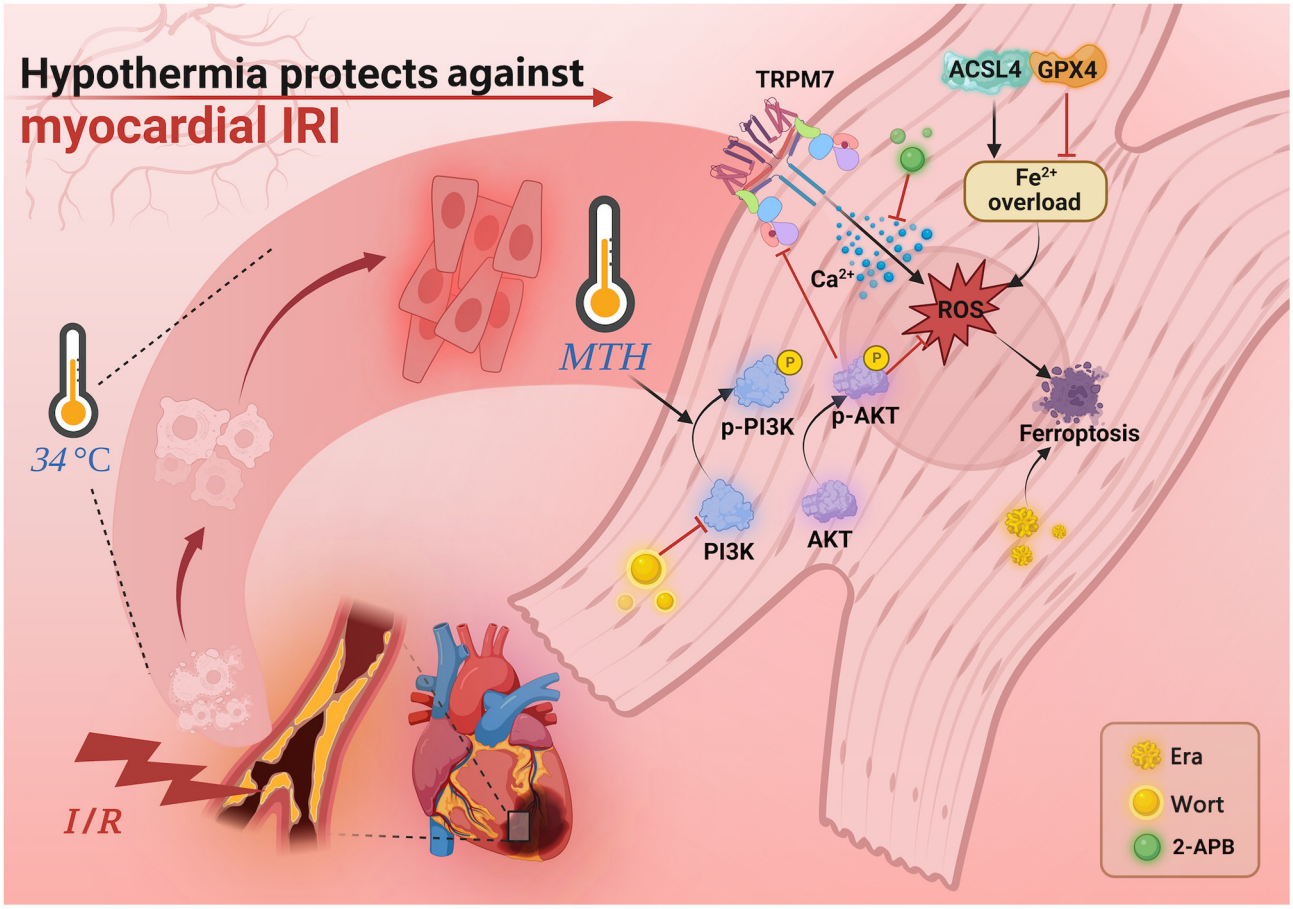


Figure 7. Protective mechanism of MTH on myocardial IRI. MTH can reduce the ferroptosis induced by myocardial I/R via inhibiting the expression of TRPM7, thereby alleviating myocardial IRI. 2-APB, 2-aminoethoxydiphenyl borate; ACSL4, acyl-CoA synthetase long chain family member 4; Era, erastin; GPX4, glutathione peroxidase 4; I/R, ischemia-reperfusion; IRI, I/R injury; MTH, mild therapeutic hypothermia; p-, phosphorylated; ROS, reactive oxygen species; TRPM7, transient receptor potential cation channel subfamily M member 7; Wort, wortmannin.

MIRI (53). Therefore, 2-APB at the same dose was used in the relevant experiments in the present study. The results demonstrated that MTH was able to inhibit the expression of TRPM7 and the occurrence of H/R-induced ferroptosis. In addition, the expression levels of TRPM7 were found to be closely associated with ferroptosis. Compared with in the I/R + MTH group, the expression levels of GPX4 in the I/R + MTH + 2-APB group were significantly increased, whereas the expression levels of ACSL4 were decreased. Notably, a previous study reported that lipopolysaccharide (LPS) induced upregulation of TRPM7 expression in cardiomyocytes, and knocking down TRPM7 could inhibit LPS-induced ferroptosis in cardiomyocytes, which was consistent with the present research findings (54).

TRPM7 serves a key role in ischemic cardiomyopathy. Inhibiting TRPM7 can exert a protective effect on the reperfusion injury of H9C2 cells and reduce the apoptotic rate of H9C2 cells (54). Under neuronal hypoxic conditions or in oxygen-glucose deprivation models, the TRPM7 channels are induced to open, causing calcium overload and inducing cells to produce large amounts of ROS, which in turn can promote the opening of TRPM7, leading to neuronal damage (28).

Ferroptosis is a type of programmed cell death characterized by iron-dependent lipid peroxidation (29). The accumulation of lipid ROS is one of the characteristics of ferroptosis. When ferroptosis occurs, large amounts of ROS are produced, which, in turn, promotes cell ferroptosis (29). GPX4 and ACSL4 have key roles in the occurrence and development of ferroptosis, and may be used as indicators to monitor ferroptosis. GPX4 has been shown to inhibit lipid peroxidation, reduce ROS production and inhibit the occurrence of cell ferroptosis (55). By contrast, ACSL4 can increase the content of phosphatidylethanolamines in cells, thereby leading to cell ferroptosis (56). Notably, a previously published study suggested that FSP1 is one of the key targets for inhibiting ferroptosis, and it is considered that FSP1-mediated ferroptosis may be independent of the GPX4-mediated ferroptosis signaling pathway (57). Therefore, GPX4 and ACSL4 were selected as the monitoring indicators of ferroptosis in the present study. As an activator of ferroptosis, our previous study (58) confirmed that 10 $\mu$M Era could effectively activate the occurrence of ferroptosis. Therefore, the same concentration of Era was chosen for the experiments performed in the present study. The expression levels of GPX4 in the I/R + MTH + 2-APB group were significantly increased compared with those in the I/R + MTH group, whereas the expression of GPX4 in the I/R + MTH + Wort group was decreased. Moreover, the expression of ACSL4 exhibited the opposite trend. In addition, several studies have indicated that ferroptosis serves a key role in cardiovascular injury caused by various diseases, including heart failure, myocardial injury

and I/R injury (30-32). Rehmannioside A has been shown to inhibit the occurrence of ferroptosis induced by I/R through activating the PI3K/AKT signaling pathway, suggesting that the PI3K/AKT signaling pathway is of crucial importance in regulating ferroptosis that is induced by I/R (33), consistent with the present experimental results. As aforementioned, according to the results from the isolated rat model and in cell experiments, the present study revealed that MTH could inhibit the expression of TRPM7 through the PI3K/AKT signaling pathway, thereby inhibiting the occurrence of ferroptosis induced by I/R and H/R, ultimately exerting a myocardial protective effect.

The present study, however, had some limitations. First, specific inhibitors were only used in the isolated rat model to study the mechanism of action of MTH. The present study did not use the C11-BODIPY method to detect lipid peroxidation levels in myocardial tissue and myocardial cells, nor was the iron ion content in myocardial tissues and cells measured. In addition, the current study did not directly manipulate the expression levels of TRPM7 using transgenic, plasmid transfection or lentiviral interference techniques, which may have confirmed that MTH could exert cardioprotective effects by manipulating the expression of TRPM7. Furthermore, the exploration of downstream sites affected by TRPM7 in ferroptosis will be an important focus of subsequent experiments. We aim to construct transgenic animal models of TRPM7, and knockdown and overexpression cell models, and explore the effects of TRPM7 on mitochondrial function and ferroptosis through molecular biology methods. Whether this mechanism can be further validated in future clinical studies, and whether it can enhance the therapeutic effect of MTH by regulating TRPM7 to inhibit ferroptosis, deserves further investigation.

The present study indicated that when MIRI occurs, the expression of TRPM7 on the myocardial cell membrane may be increased. As a non-selective cation channel, TRPM7 is permeable to calcium and magnesium ions in the plasma. As its expression level is increased, this may lead to calcium ion influx, causing calcium overload of myocardial cells and, finally, myocardial cell damage. In addition, calcium overload is positively associated with a large amount of ROS accumulation produced by myocardial cells, further causing myocardial damage. It is worth noting that the accumulation of ROS can induce ferroptosis, and further aggravate myocardial injury. Therefore, it may be suggested that MTH therapy inhibits the expression of TRPM7 through activating the PI3K/AKT signaling pathway, thereby inhibiting the occurrence of ferroptosis, ultimately participating in myocardial protection (Fig. 7). In conclusion, MTH protection activates the PI3K/AKT signaling pathway to inhibit TRPM7 and suppress ferroptosis induced by MIRI. However, further studies are required to investigate the clinical application of MTH.

## Acknowledgements

Not applicable.

## Funding

This work was supported by the National Natural Science Foundation of China (grant no. 82160371 to JZ, grant no. 81760338 to SY); the Key Projects of Jiangxi Provincial Department of Education Science and Technology Plan (grant no. GJJ210134 to SY); the Natural Science Foundation in Jiangxi Province grant (grant no. 20224ACB216009 to JZ); the Science and Technology Plan of Jiangxi Provincial Administration of Traditional Chinese Medicine (grant no. 2022B1038 to YQL); and the Science and Technology Plan of Jiangxi Provincial Health Commission (grant no. 202310106 to YQL).

## Availability of data and materials

The data generated in the present study may be requested from the corresponding author.

## Authors' contributions

YQL, YXC, PY, DJZ, XYT, ZCZ, FX, WD, YL and ZYT performed nearly all of the experiments. YQL, YXC, PY and JZ analyzed the data. YQL, YXC, PY, JZ and SY designed the study and all of the experiments were performed under their guidance. YXC, PY and DJZ were the major contributors in writing the manuscript. YQL and SY confirm the authenticity of all the raw data. All authors read and approved the final version of the manuscript.

## Ethics approval and consent to participate

The Animal Experiment Ethics Committee of Nanchang University provided full approval for this research (no. NCULAE-20221121086). In addition, this study also followed the Animal Research: Reporting *In Vivo* Experiments Guidelines and the American Veterinary Medical Association Euthanasia Guidelines 2020.

## Patient consent for publication

Not applicable.

## Competing interests

The authors declare they have no competing interests.

## References

1. Petrie MC, Verma S, Docherty KF, Inzucchi SE, Anand I, Belohlávek J, Böhm M, Chiang CE, Chopra VK, de Boer RA, *et al*: Effect of dapagliflozin on worsening heart failure and cardiovascular death in patients with heart failure with and without diabetes. JAMA 323: 1353-1368, 2020.
2. Raphael CE, Roger VL, Sandoval Y, Singh M, Bell M, Lerman A, Rihal CS, Gersh BJ, Lewis B, Lennon RJ, *et al*: Incidence, trends, and outcomes of type 2 myocardial infarction in a community cohort. Circulation 141: 454-463, 2020.
3. Chang X, Toan S, Li R and Zhou H: Therapeutic strategies in ischemic cardiomyopathy: Focus on mitochondrial quality surveillance. EBioMedicine 84: 104260, 2022.
4. Wang K, Li Y, Qiang T, Chen J and Wang X: Role of epigenetic regulation in myocardial ischemia/reperfusion injury. Pharmacol Res 170: 105743, 2021.
5. Algoet M, Janssens S, Himmelreich U, Gsell W, Pusovnik M, Van den Eynde J and Oosterlinck W: Myocardial ischemia-reperfusion injury and the influence of inflammation. Trends Cardiovasc Med 33: 357-366, 2023.

6. Zhao WK, Zhou Y, Xu TT and Wu Q: Ferroptosis: Opportunities and challenges in myocardial ischemia-reperfusion injury. Oxid Med Cell Longev 2021: 9929687, 2021.
7. Chen CL, Zhang L, Jin Z, Kasumov T and Chen YR: Mitochondrial redox regulation and myocardial ischemia-reperfusion injury. Am J Physiol Cell Physiol 322: C12-C23, 2022.
8. Mokhtari-Zaer A, Marefati N, Atkin SL, Butler AE and Sahebkar A: The protective role of curcumin in myocardial ischemia-reperfusion injury. J Cell Physiol 234: 214-222, 2018.
9. Ibáñez B, Heusch G, Ovize M and Van de Werf F: Evolving therapies for myocardial ischemia/reperfusion injury. J Am Coll Cardiol 65: 1454-1471, 2015.
10. Sessler DI: Mild perioperative hypothermia. N Engl J Med 336: 1730-1737, 1997.
11. Shi H, Su Z, Su H, Chen H, Zhang Y and Cheng Y: Mild hypothermia improves brain injury in rats with intracerebral hemorrhage by inhibiting IRAK2/NF-κB signaling pathway. Brain Behav 11: e01947, 2021.
12. Iaizzo PA, Kehler CH, Carr RJ, Sessler DI and Belani KG: Prior hypothermia attenuates malignant hyperthermia in susceptible swine. Anesth Analg 82: 803-809, 1996.
13. Wass CT, Lanier WL, Hofer RE, Scheithauer BW and Andrews AG: Temperature changes of > or=1 degree C alter functional neurologic outcome and histopathology in a canine model of complete cerebral ischemia. Anesthesiology 83: 325-335, 1995.
14. Schleef M, Gonnot F, Pillot B, Leon C, Chanon S, Vieille-Marchiset A, Rabeyrin M, Bidaux G, Guebre-Egziabher F, Juillard L, *et al*: Mild Therapeutic hypothermia protects from acute and chronic renal ischemia-reperfusion injury in mice by mitigated mitochondrial dysfunction and modulation of local and systemic inflammation. Int J Mol Sci 23: 9229, 2022.
15. Liu X, Wen S, Zhao S, Yan F, Zhao S, Wu D and Ji X: Mild therapeutic hypothermia protects the brain from ischemia/reperfusion injury through upregulation of iASPP. Aging Dis 9: 401-411, 2018.
16. Xiao Q, Ye Q, Wang W, Xiao J, Fu B, Xia Z, Zhang X, Liu Z and Zeng X: Mild hypothermia pretreatment protects against liver ischemia reperfusion injury via the PI3K/AKT/FOXO3a pathway. Mol Med Rep 16: 7520-7526, 2017.
17. Tissier R, Chenoune M, Ghaleb B, Cohen MV, Downey JM and Berdeaux A: The small chill: Mild hypothermia for cardioprotection? Cardiovasc Res 88: 406-414, 2010.
18. Kanemoto S, Matsubara M, Noma M, Leshnower BG, Parish LM, Jackson BM, Hinmon R, Hamamoto H, Gorman JH III and Gorman RC: Mild hypothermia to limit myocardial ischemia-reperfusion injury: Importance of timing. Ann Thorac Surg 87: 157-163, 2009.
19. Mochizuki T, Yu S, Katoh T, Aoki K and Sato S: Cardioprotective effect of therapeutic hypothermia at 34°C against ischaemia/reperfusion injury mediated by PI3K and nitric oxide in a rat isolated heart model. Resuscitation 83: 238-242, 2012.
20. Gao R, Zhao H, Wang X, Tang B, Cai Y, Zhang X, Zong H, Li Y and Wang Y: Mild hypothermia therapy lowers the inflammatory level and apoptosis rate of myocardial cells of rats with myocardial ischemia-reperfusion injury via the NLRP3 inflammasome pathway. Comput Math Methods Med 2021: 6415275, 2021.
21. Harteneck C, Plant TD and Schultz G: From worm to man: Three subfamilies of TRP channels. Trends Neurosci 23: 159-166, 2000.
22. Sah R, Mesirca P, Mason X, Gibson W, Bates-Withers C, Van den Boogert M, Chaudhuri D, Pu WT, Mangoni ME and Clapham DE: Timing of myocardial trpm7 deletion during cardiogenesis variably disrupts adult ventricular function, conduction, and repolarization. Circulation 128: 101-114, 2013.
23. Zhao L, Wang Y, Sun N, Liu X, Li L and Shi J: Electroacupuncture regulates TRPM7 expression through the trkA/PI3K pathway after cerebral ischemia-reperfusion in rats. Life Sci 81: 1211-1222, 2007.
24. Aarts M, Iihara K, Wei WL, Xiong ZG, Arundine M, Cerwinski W, MacDonald JF and Tymianski M: A key role for TRPM7 channels in anoxic neuronal death. Cell 115: 863-877, 2003.
25. Fatima G, Sharma VP, Das SK and Mahdi AA: Oxidative stress and antioxidative parameters in patients with spinal cord injury: Implications in the pathogenesis of disease. Spinal Cord 53: 3-6, 2015.
26. Meng Z, Wang X, Yang Z and Xiang F: Expression of transient receptor potential melastatin 7 up-regulated in the early stage of renal ischemia-reperfusion. Transplant Proc 44: 1206-1210, 2012.
27. Zhou DM, Sun LL, Zhu J, Chen B, Li XQ and Li WD: MiR-9 promotes angiogenesis of endothelial progenitor cell to facilitate thrombi recanalization via targeting TRPM7 through PI3K/Akt/autophagy pathway. J Cell Mol Med 24: 4624-4632, 2020.
28. Yang J, Hu S, Huang L, Zhou J, Xiang H, Yang H, Cheng H and Tang Y: Protective effect of inhibiting TRPM7 expression on hypoxia post-treatment H9C2 cardiomyocytes. Clin Hemorheol Microcirc 77: 91-105, 2021.
29. Dixon SJ, Lemberg KM, Lamprecht MR, Skouta R, Zaitsev EM, Gleason CE, Patel DN, Bauer AJ, Cantley AM, Yang WS, *et al*: Ferroptosis: An iron-dependent form of nonapoptotic cell death. Cell 149: 1060-1072, 2012.
30. Mou Y, Wang J, Wu J, He D, Zhang C, Duan C and Li B: Ferroptosis, a new form of cell death: Opportunities and challenges in cancer. J Hematol Oncol 12: 34, 2019.
31. Su LJ, Zhang JH, Gomez H, Murugan R, Hong X, Xu D, Jiang F and Peng ZY: Reactive oxygen species-induced lipid peroxidation in apoptosis, autophagy, and ferroptosis. Oxid Med Cell Longev 2019: 5080843, 2019.
32. Wu X, Li Y, Zhang S and Zhou X: Ferroptosis as a novel therapeutic target for cardiovascular disease. Theranostics 11: 3052-3059, 2021.
33. Zhang Z, Tang J, Song J, Xie M, Liu Y, Dong Z, Liu X, Li X, Zhang M, Chen Y, *et al*: Elabela alleviates ferroptosis, myocardial remodeling, fibrosis and heart dysfunction in hypertensive mice by modulating the IL-6/STAT3/GPX4 signaling. Free Radic Biol Med 181: 130-142, 2022.
34. Wang X, Chen X, Zhou W, Men H, Bao T, Sun Y, Wang Q, Tan Y, Keller BB, Tong Q, *et al*: Ferroptosis is essential for diabetic cardiomyopathy and is prevented by sulforaphane via AMPK/NRF2 pathways. Acta Pharm Sin B 12: 708-722, 2022.
35. Sun L, Wang H, Xu D, Yu S, Zhang L and Li X: Lapatinib induces mitochondrial dysfunction to enhance oxidative stress and ferroptosis in doxorubicin-induced cardiomyocytes via inhibition of PI3K/AKT signaling pathway. Bioengineered 13: 48-60, 2022.
36. Shi R, Fu Y, Zhao D, Boczek T, Wang W and Guo F: Cell death modulation by transient receptor potential melastatin channels TRPM2 and TRPM7 and their underlying molecular mechanisms. Biochem Pharmacol 190: 114664, 2021.
37. Hickman DL: Euthanasia of neonatal rats and mice using carbon monoxide. J Am Assoc Lab Anim Sci 62: 274-278, 2023.
38. Montaigne D, Marechal X, Modine T, Coisne A, Mouton S, Fayad G, Ninni S, Klein C, Ortmans S, Seunes C, *et al*: Daytime variation of perioperative myocardial injury in cardiac surgery and its prevention by Rev-Erbα antagonism: a single-centre propensity-matched cohort study and a randomised study. Lancet 391: 59-69, 2018.
39. Lian ZX, Wang F, Fu JH, Chen ZY, Xin H and Yao RY: ATP-induced cardioprotection against myocardial ischemia/reperfusion injury is mediated through the RISK pathway. Exp Ther Med 12: 2063-2068, 2016.
40. Ma X, Godar RJ, Liu H and Diwan A: Enhancing lysosome biogenesis attenuates BNIP3-induced cardiomyocyte death. Autophagy 8: 297-309, 2012.
41. Moon BF, Iyer SK, Hwuang E, Solomon MP, Hall AT, Kumar R, Josselyn NJ, Higbee-Dempsey EM, Tsourkas A, Imai A, *et al*: Iron imaging in myocardial infarction reperfusion injury. Nat Commun 11: 3273, 2020.
42. Götberg M, Olivecrona GK, Koul S, Carlsson M, Engblom H, Ugander M, van der Pals J, Algotsson L, Arheden H and Erlinge D: A pilot study of rapid cooling by cold saline and endovascular cooling before reperfusion in patients with ST-elevation myocardial infarction. Circ Cardiovasc Interv 3: 400-407, 2010.
43. Hamamoto H, Leshnower BG, Parish LM, Sakamoto H, Kanemoto S, Hinmon R, Miyamoto S, Gorman JH III and Gorman RC: Regional heterogeneity of myocardial reperfusion injury: Effect of mild hypothermia. Ann Thorac Surg 87: 164-171, 2009.
44. Jung KT, Bapat A, Kim YK, Hucker WJ and Lee K: Therapeutic hypothermia for acute myocardial infarction: A narrative review of evidence from animal and clinical studies. Korean J Anesthesiol 75: 216-230, 2022.
45. Qin Z, Shen S, Qu K, Nie Y and Zhang H: Mild hypothermia in rat with acute myocardial ischaemia-reperfusion injury complicating severe sepsis. J Cell Mol Med 25: 6448-6454, 2021.

46. Maynard C, Longstreth WT Jr, Nichol G, Hallstrom A, Kudenchuk PJ, Rea T, Copass MK, Carlbom D, Deem S, Olsufka M, *et al*: Effect of prehospital induction of mild hypothermia on 3-month neurological status and 1-year survival among adults with cardiac arrest: Long-term follow-up of a randomized, clinical trial. J Am Heart Assoc 4: e001693, 2015.
47. Fuernau G, Beck J, Desch S, Eitel I, Jung C, Erbs S, Mangner N, Lurz P, Fengler K, Jobs A, *et al*: Mild Hypothermia in Cardiogenic Shock Complicating Myocardial Infarction. Circulation 139: 448-457, 2019.
48. Karar J and Maity A: PI3K/AKT/mTOR pathway in angiogenesis. Front Mol Neurosci 4: 51, 2011.
49. Sánchez-Alegría K, Flores-León M, Avila-Muñoz E, Rodríguez-Corona N and Arias C: PI3K signaling in neurons: A central node for the control of multiple functions. Int J Mol Sci 19: 3725, 2018.
50. Di-Luoffo M, Ben-Meriem Z, Lefebvre P, Delarue M and Guillermet-Guibert J: PI3K functions as a hub in mechanotransduction. Trends Biochem Sci 46: 878-888, 2021.
51. Ghigo A and Li M: Phosphoinositide 3-kinase: Friend and foe in cardiovascular disease. Front Pharmacol 6: 169, 2015.
52. Yu D, Xiong J, Gao Y, Li J, Zhu D, Shen X, Sun L and Wang X: Resveratrol activates PI3K/AKT to reduce myocardial cell apoptosis and mitochondrial oxidative damage caused by myocardial ischemia/reperfusion injury. Acta Histochemica 123: 151739, 2021.
53. Shen YC, Shen YJ, Lee WS, Chen MYC, Tu WC and Yang KT: Two benzene rings with a boron atom comprise the core structure of 2-APB responsible for the anti-oxidative and protective effect on the ischemia/reperfusion-induced rat heart injury. Antioxidants (Basel) 10: 1667, 2021.
54. Deng W, Ren G, Luo J, Gao S, Huang W, Liu W and Ye S: TRPM7 mediates endoplasmic reticulum stress and ferroptosis in sepsis-induced myocardial injury. J Bioenerg Biomembr 55: 207-217, 2023.
55. Ursini F and Maiorino M: Lipid peroxidation and ferroptosis: The role of GSH and GPx4. Free Radic Biol Med 152: 175-185, 2020.
56. Doll S, Proneth B, Tyurina YY, Panzilius E, Kobayashi S, Ingold I, Irmler M, Beckers J, Aichler M, Walch A, *et al*: ACSL4 dictates ferroptosis sensitivity by shaping cellular lipid composition. Nat Chem Biol 13: 91-98, 2017.
57. Bersuker K, Hendricks JM, Li Z, Magtanong L, Ford B, Tang PH, Roberts MA, Tong B, Maimone TJ, Zoncu R, *et al*: The CoQ oxidoreductase FSP1 acts parallel to GPX4 to inhibit ferroptosis. Nature 575: 688-692, 2019.
58. Yu P, Zhang J, Ding Y, Chen D, Sun H, Yuan F, Li S, Li X, Yang P, Fu L, *et al*: Dexmedetomidine post-conditioning alleviates myocardial ischemia-reperfusion injury in rats by ferroptosis inhibition via SLC7A11/GPX4 axis activation. Hum Cell 35: 836-848, 2022.